Geophysical Research Letters

RESEARCH LETTER
10.1029/2020GL090661

Special Section:
Advancing prediction of coastal marine ecosystems

The Continuum of Northeast Pacific Marine Heatwaves and Their Relationship to the Tropical Pacific

Tongtong Xu[1], Matthew Newman[2,3], Antonietta Capotondi[2,3], and Emanuele Di Lorenzo[4]

[1]School of Civil and Environmental Engineering, Georgia Institute of Technology, Atlanta, GA, USA, [2]CIRES, University of Colorado, Boulder, CO, USA, [3]NOAA Physical Sciences Laboratory, Boulder, CO, USA, [4]Program in Ocean Science and Engineering, Georgia Institute of Technology, Atlanta, GA, USA

Abstract Some questions remain concerning the record-breaking 2013–2015 Northeast Pacific marine heatwave (MHW) event: was it exceptional or merely the most pronounced of a group of similar events, and was its intensity and multiyear duration driven by internal extratropical processes or did the tropics play an important role? By analyzing the statistical behavior of the historical MHWs within the ERSST.v3 data set over the 1950–2019 period, we find that Northeast Pacific MHWs occurred over a continuum of intensities and durations, suggesting that these events are a recurrent Pacific phenomenon. These statistics and corresponding composite evolution are dynamically reproduced by a large ensemble simulation of a Pacific Linear Inverse Model, thereby providing a greater range of MHW expressions than the short observational record alone. Consistent with the 2013–2015 event's evolution, we find that overall the tropics influence MHWs primarily by increasing their duration, while MHW intensity is related to the initial extratropical anomalies.

Plain Language Summary Marine heatwaves (MHWs), analogous to heatwaves on land, describe when the ocean temperature is abnormally warm for a prolonged period. In the Northeast Pacific during 2013–2015, an exceptionally strong and long-lasting MHW occurred causing destructive ecosystem impacts including massive mortality of fish and birds. Given the unusual nature of the event, it is of considerable interest to ask whether it occurred largely naturally or whether it might have been impacted by climate change. To address this question, we analyze historical MHWs over the 1950–2019 period and, since there may have been too few observed MHWs for comprehensive scientific understanding, additionally construct a statistical model mimicking how Pacific ocean surface temperatures evolve over time. In this manner, we create 2,000 "alternate histories" of what could have happened over the 1950–2019 period to provide enough MHWs for further analysis. Our findings suggest that Northeast Pacific MHWs are an irregularly recurring natural phenomenon, whose duration is largely dependent on interactions with the remote tropical Pacific but whose intensity depends primarily on local conditions within the North Pacific. A 2013–2015 event could well have occurred without climate change, but our model cannot entirely anticipate its prolonged severity.

Key Points:

- Prolonged and intense marine heatwaves (MHWs) are a recurrent Northeast Pacific phenomenon, well captured by a simple Linear Inverse Model
- Northeast Pacific MHW duration appears greatly affected by tropical interactions, while MHW intensity stems primarily from the extratropics
- The 2013–2015 Northeast Pacific MHW was an extreme example of this phenomenon that may have been further strengthened by climate change

Supporting Information:

- Supporting Information S1

Correspondence to:
T. Xu,
txu68@gatech.edu

Citation:
Xu, T., Newman, M., Capotondi, A., & Di Lorenzo, E. (2021). The Continuum of Northeast Pacific Marine Heatwaves and Their Relationship to the Tropical Pacific. *Geophysical Research Letters*, *48*, e2020GL090661. https://doi.org/10.1029/2020GL090661

Received 3 SEP 2020
Accepted 10 DEC 2020

1. Introduction

Marine heatwaves (MHWs) are extended periods of anomalously warm ocean temperatures and are often classified based on their intensity and duration (Hobday et al., 2016, 2018). The most prolonged MHW of the past 70 years, occurring during 2013–2015, covered a broad region of the Northeast Pacific, with local maximum warming of 2.8°C (Bond et al., 2015; Di Lorenzo & Mantua, 2016), and did not end until after the development in the tropics of a strong El Niño. Its ecosystem impacts were unprecedented, including massive stranding, entanglement, and mortality of marine species and seabirds (Cavole et al., 2016; Jones et al., 2018; Santora et al., 2020) and prolonged harmful algal blooms that closed major fisheries (McCabe et al., 2016; Ryan et al., 2017; Sanford et al., 2019). This record-breaking event led to enhanced scrutiny of many Northeast Pacific MHW aspects (Frolicher & Laufkotter, 2018; Holbrook et al., 2020), including their severities (Hobday et al., 2016; Jacox et al., 2020; Scannell et al., 2016), tropical and extratropical driving mechanisms (D. J. Amaya et al., 2020; Bond et al., 2015; Di Lorenzo & Mantua, 2016; Holbrook et al., 2019), and predictability (Hu et al., 2017; Jacox et al. 2019).

Despite the record-breaking nature of the 2013–2015 event, there have been other intense Northeast Pacific warm events before and since (e.g., D. Amaya et al., 2016; D. J. Amaya et al., 2020; Oliver et al., 2018). In fact, prolonged oceanic warm events occur over a range of intensities and durations (Scannell et al., 2016). However, the observational record may be too short either to represent the full spectrum of possible MHWs or to differentiate what drives variations in MHW intensity and duration, including the relative roles of tropical and extratropical processes.

We suggest that Northeast Pacific MHWs may be viewed as a recurrent phenomenon of the Pacific basin involving large-scale teleconnection dynamics, with the 2013–2015 MHW being a particularly strong realization within a continuum of MHW events. In this view, MHWs are neither unprecedented nor intrinsically unpredictable in their dynamical evolutions, although some properties like maximum amplitude may be (Hu et al., 2017). To demonstrate this, we diagnose Northeast Pacific MHWs using a Pacific-basin Linear Inverse Model (LIM) (Penland & Sardeshmukh, 1995), an empirical–dynamical model derived from observed anomaly covariances. The LIM is attractive for this purpose since it captures observed climate anomaly evolution over extended periods (e.g., its seasonal forecasts are generally comparable with state-of-the-art multimodel operational forecast; Newman & Sardeshmukh, 2017), yet its low dimensionality allows generation of long climate simulations suitable for hypothesis testing (e.g., Capotondi & Sardeshmukh, 2017; Newman, Shin, et al., 2011). Here, we develop a LIM to produce a large ensemble simulation of tropical and North Pacific sea surface temperature (SST) anomalies (SSTa), so that we may evaluate observed MHW evolution against the much larger sample of simulated MHW events.

2. Data and Methods

2.1. Data

Monthly SST data from the 1950–2019 period were obtained from the National Oceanic and Atmospheric Administration (NOAA) Extended Reconstruction SST, version 3 (ERSST.v3b; Smith et al. [2008]). SSTa were constructed by temporally smoothing SST with a 3-month running mean, removing the monthly climatology, and linearly detrending. The spatial resolution of SSTa was 2° × 2°.

2.2. LIM Climate Simulations

Numerous studies have shown how LIMs, stochastically-forced linear dynamical models constructed from observations, realistically capture observed Pacific ocean seasonal anomaly evolution (e.g., Alexander et al., 2008; Dias et al., 2019; Newman et al., 2016; Penland & Sardeshmukh, 1995; see also Newman & Sardeshmukh, 2017 and references therein). The LIM is expressed as

$$\frac{d\mathbf{x}}{dt} = \mathbf{L}\mathbf{x} + \boldsymbol{\xi}, \tag{1}$$

where the state vector $\mathbf{x}(t)$ is the climate anomaly, $\mathbf{L}$ is a linear dynamical operator, $\boldsymbol{\xi}$ is a vector of temporally white noise, and t is time. This simple linear model can be relevant when nonlinear processes act more rapidly than linear processes (Hasselmann, 1976), such as when weather forces more slowly evolving oceanic mixed layer thermal anomalies (Frankignoul & Hasselmann, 1977).

In this paper, $\mathbf{x}(t)$ represents SSTa within the region 110°E–60°W and 20°S–60°N. (Detailed LIM construction is in the Supplemental Material; see also Penland and Sardeshmukh [1995].) Although fully capturing interannual-to-decadal SSTa variability requires including some measure of upper ocean heat content (e.g., Newman, Alexander, et al., 2011), our SST-only model captures the dominant seasonal climate dynamics of interest here (Penland & Sardeshmukh, 1995), as the LIM predicts lag-covariance statistics that match observations over 6–12 months lags (Figure S1).

Since the LIM is a dynamical model, lengthy climate simulations may be generated by integrating Equation 1 forwards in time, driven by white noise forcing with observationally constrained spatial structure (see Supplemental Material for detailed stochastic integration; see also Penland and Matrosova [1994]). In this manner, we generated a 2,000-member ensemble of 70-year-long segments; each may be considered an "alternate history" of the past 70 years. This ensemble is analogous to other complex coupled climate

model "large ensemble" simulations, used to explore common elements of observed climate phenomena such as El Niño-southern oscillation (ENSO) (e.g., Deser et al., 2018) and their potential dependence on small available sample size. Similarly, we compare the relatively few observed MHW events to the large number of simulated events in our ensemble, which all evolve consistent with observed dynamics and so *could* have occurred (e.g., Newman, Shin, et al., 2011). Our large ensemble also allows determination of those aspects of observed MHWs that the LIM cannot capture. We note again that this ensemble represents the detrended SSTa; that is, we assume climate change drives the trend but does not otherwise significantly impact detrended SSTa evolution.

3. Recurrence and Evolution of Northeast Pacific MHWs in Observations and LIM

3.1. Composite Analysis of Observed Northeast Pacific MHWs

To diagnose Northeast Pacific MHWs, including their observed and simulated evolution, we defined a Northeast Pacific ("NEPac") index (Figure 1(a)) by averaging SSTa within a representative region (150°W–135°W, 35°N–46°N; inset in Figure 1(a)), our results were insensitive to this choice (also see discussion of Figure 1(d)). Following previous studies of oceanic (Hobday et al., 2016; Holbrook et al., 2019; Scannell et al., 2016) and atmospheric (e.g., Dole & Gordon, 1983; Miller et al., 2020) persistent anomalies, prolonged anomalously warm events were identified when the NEPac index exceeded a given temperature amplitude threshold ("intensity") and persisted above it for a given length of time ("duration"). Following these and similar studies, we calculated the Intensity–Duration–Frequency (IDF) plot (Figure 1(b)), which shows the frequency of anomalously warm events for varying intensity and duration thresholds. For example, extremely warm events persisting for a short period are about as frequent as more prolonged but weaker events.

We also examined sensitivity to the region chosen for the NEPac index. The mean duration of abnormally warm events ($\geq 1\sigma$) at each location within Northeast Pacific was 4–6 months (Figure 1(d)). That is, the mean persistence of abnormally warm events in the Northeast Pacific is not too sensitive to the location, so MHW duration may be represented using our NEPac index.

If we define Northeast Pacific MHWs by choosing events staying above the 1σ intensity threshold at least 5 months (blue circle in Figure 1(b)), there are 12 discrete MHW events over the past 70 years (gray bars in Figure 1(a) and Table S1). Their composite evolution is shown in Figure 1(e). At $t = -12$ months (Figure 1(e1)), the composite spatial pattern shows warm temperature anomalies extending zonally along 40°N within the central North Pacific Current region. These warm anomalies extended eastward at $t = -6$ months (Figure 1(e2)), intensifying until the NEPac index reached the 1σ threshold at $t = 0$ months (Figure 1(e3)). While the Northeast Pacific warming persisted at $t = +6$ months (Figure 1(e4)), El Niño conditions developed in the tropics, perhaps linked to the Northeast Pacific warming through the North Pacific Meridional Mode (NPMM) (Chiang & Vimont, 2004) that is often identified as an ENSO precursor (Capotondi & Sardeshmukh, 2015; Larson & Kirtman, 2014). At $t = +12$ months (Figure 1(e5)), while El Niño persisted, the Northeast Pacific warming spread along the US West Coast, consistent with atmospheric teleconnections from the tropics (Alexander et al., 2002; Di Lorenzo & Mantua, 2016).

Note that the 1σ-intensity/5-month-duration criterion splits the 2013–2015 MHW into three "events" (gray bars in Figure 1(a) and Table S1). We tested whether the composite may be overly dominated by these events, first by excluding all events occurring after 2012 from the composite, and then adding them back (Figure S2), finding little impact on the composite MHW progression.

Figure 1(b) suggests no obvious, unique definition of an MHW event. Hobday et al. (2016) proposed using the 90th percentile ($\sim 1.3\sigma$) intensity threshold. One concern with the higher threshold is that it halves the number of samples; to obtain the same sample size requires lowering the duration threshold to 3 months (Figure S3(b)). We chose instead to reduce the intensity threshold while maintaining a longer duration threshold. Still, the evolution of both composites is generally similar (Figure S3(e)), apart from the somewhat longer duration in our composite (Figure 1(e)), suggesting that our results are not sensitive to this choice.

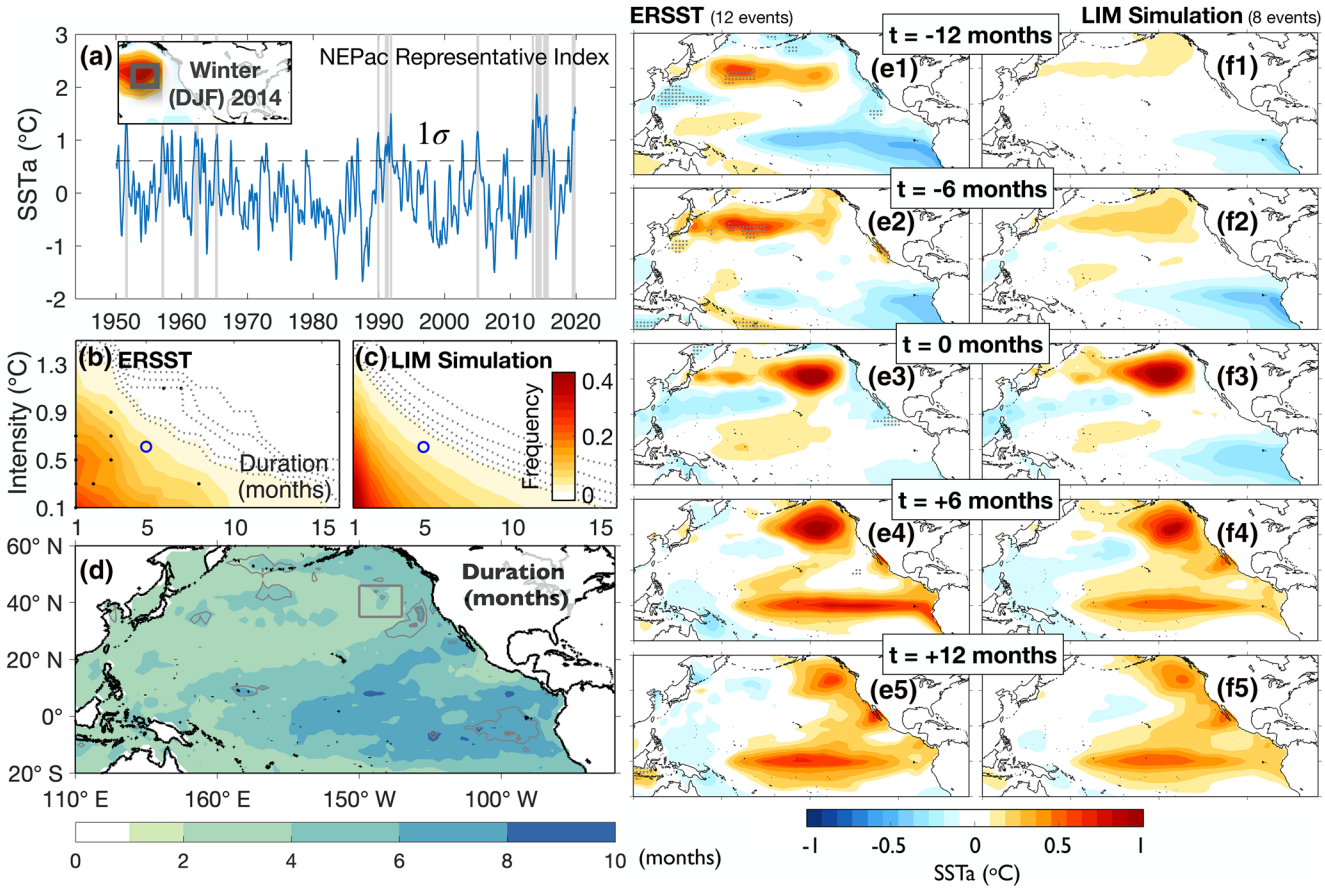

Figure 1. Statistics and evolution of composite Northeast Pacific marine heatwaves (MHWs) from observations and Linear Inverse Model (LIM) simulation. (a) Northeast Pacific (NEPac) index, defined as the spatially averaged SST anomalies (SSTa) within the gray box (in the insert overlaid on the winter 2014 SSTa; in (d)). Gray bars mark events that both exceeded one standard deviation (1σ) and persisted for ≥5 months. Dashed line marks the 1σ intensity. (b, c) Intensity–Duration–Frequency (IDF) plot derived from the (b) observed and (c) LIM-simulated NEPac time series, obtained by calculating the number of events exceeding each intensity and duration threshold pair. Dashed lines represent frequency contours from 0.005 to 0.025 with an increment of 0.005. In (b), dots mark observed values that are 95% significantly different from LIM. (d) Average duration (in months) of warm events exceeding 1σ calculated at each grid point of our domain. Shading denotes the observed average duration. Results of LIM simulation are generally similar except in the regions enclosed by gray contours (at a 95% significance level). (e1-e5, f1-f5) Composite Northeast Pacific MHW evolution based on (e) observations and (f) LIM simulation. The composite at $t = 0$ months is calculated by averaging SSTa of all events, defined when the NEPac index first exceeds 1σ and subsequently persists for at least 5 months. This pair of intensity and duration thresholds is indicated by the blue circles in (b) and (c). Other maps represent lead and lag composites at $t = \pm 6, \pm 12$ months. Gray dots in (e) show where the observed composite amplitude is 95% significantly different from the LIM simulation. Number of events inserted in (e, f) represents mean events per 70 years.

3.2. Comparison to the LIM Simulation

We next evaluate how well observed MHWs are reproduced within the LIM simulation. The IDF plot derived from the LIM-simulated NEPac time series (Figure 1(c)) matches the observed IDF plot (Figure 1(b)), except for, for example, short (1–3 months) duration MHWs where the LIM event frequencies were 95% significantly different from the observed (black dots in Figure 1(b); see Supplemental Material for significance tests), perhaps due to the 3-month running mean anomalies used to construct the LIM. Similarly, the mean duration of abnormally warm events (≥1σ) within the LIM simulation generally agrees well with observations, except for some small regions indicated by gray dots in Figure 1(d). More generally, probability distribution and lag covariability statistics of the NEPac index derived from the LIM simulation are consistent with observations (Figure S4). In sum, the LIM simulation reproduces the statistics of observed MHWs over a continuum of intensities and durations, implying that it captures key MHW dynamics consistent with observations.

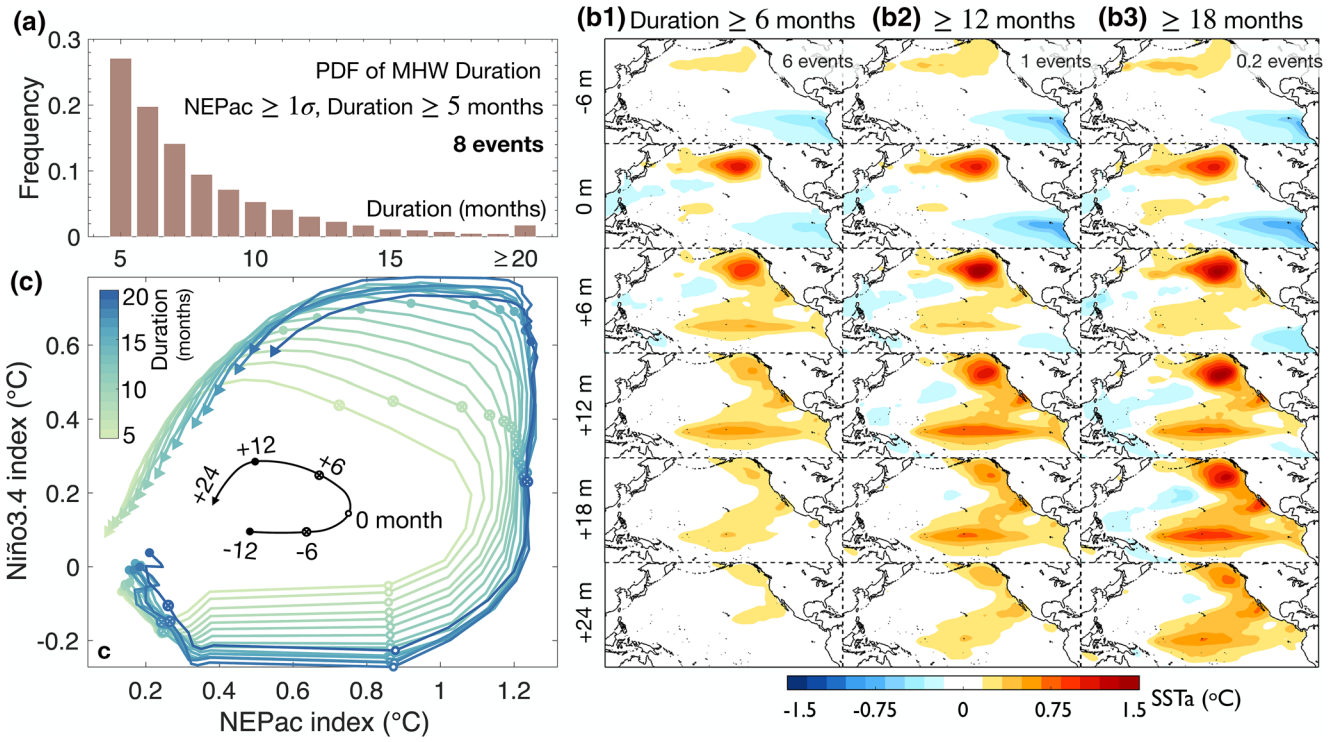

Figure 2. Statistics and evolution of LIM-simulated Northeast Pacific MHW composites with varying duration thresholds, and their relationship to ENSO variability, for fixed intensity threshold 1σ. (a) Probability distribution function (PDF) of durations for MHW events exceeding an intensity of 1σ, starting at 5-month duration. (b) Composite evolution of Northeast Pacific MHWs with varying duration thresholds: (b1) 6 months, (b2) 12 months, and (b3) 18 months, all exceeding an intensity of 1σ. Composite evolution from 6 months before to 24 months after the MHW initiation. (c) Niño 3.4 index as a function of NEPac index during the composite evolution of Northeast Pacific MHWs, from −12 months to +24 months, where each line represents varying duration thresholds ranging from 5 months (light green) to 20 months (blue). Number of events inserted in (a) and (b) represents mean events per 70 years.

Composite evolution of the LIM-simulated MHWs (Figures 1(f1)–1(f5)) also matches observations (Figures 1(e1)–1(e5)). The most notable difference is the LIM's significantly weaker amplitude in the Northwest Pacific before $t = 0$ months. Other differences (e.g., in the Tropics prior to and at onset) are not 95% statistically significant, tested against a Monte Carlo analysis of the LIM ensemble (see Supplemental Material). On average, the ensemble LIM simulation contained about 8 MHW events for each 70-year-long ensemble member, compared to 12 historical events over the past 70 years (with 11.1% of the 70-year-long realizations having ≥12 events). Overall, the similar evolution between the observed and the simulated MHW composites suggests that MHWs, as a phenomenon, share some common features in their evolution and that these prolonged and spatially evolving warm events recur in the Pacific basin.

4. Characteristics of Northeast Pacific MHWs Linked to the Tropical Pacific

In this section, we identify how differing tropical and extratropical dynamical contributions drive the continuum of MHWs captured by Figure 1(c). To do this, we explore the sensitivity of LIM composite MHWs to different intensity and duration thresholds, by comparing composites where we vary one threshold while fixing the other.

Figure 2 shows the sensitivity to duration, with intensity fixed at 1σ. The probability distribution function (PDF) of durations from all simulated MHW events exceeding the 1σ intensity threshold and persisting at least 5 months (Figure 2(a)) shows a notable fraction of long-lived MHWs (up to 53 months) in the LIM simulation. From these simulated events, composite MHW evolution was determined for subsets with durations ≥6 months (Figure 2(b1)), ≥12 months (Figure 2(b2)), and ≥18 months (Figure 2(b3)). We found three key differences for longer versus shorter duration thresholds: (1) while the MHW onset intensity was

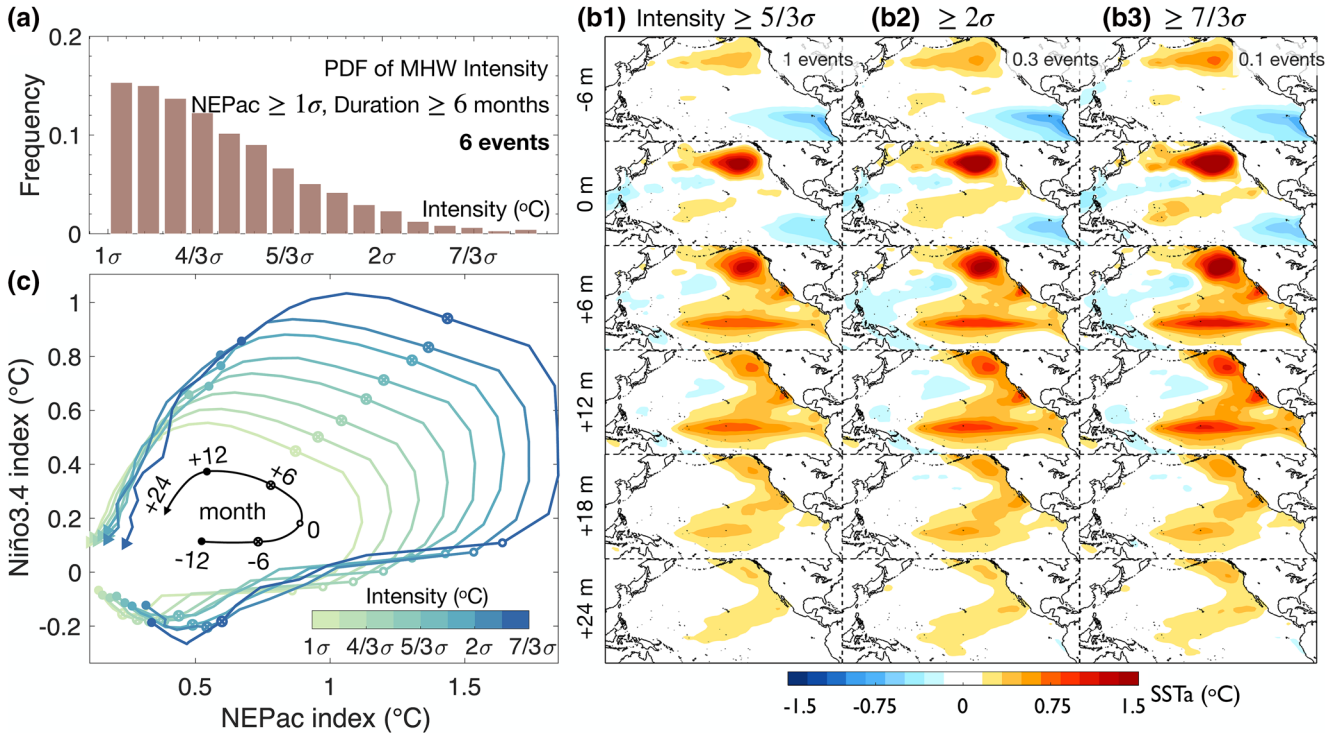

Figure 3. Same as Figure 2, except for varying intensity thresholds for a fixed 6-month duration threshold.

similar regardless of the duration thresholds, the maximum MHW amplitude was greater for longer-lasting MHWs, (2) the initial equatorial Pacific cold anomalies were stronger and persisted longer, and (3) the central Pacific El Niño was slower to develop, reaching greater peak amplitude at later lags (cf., $t = +12$ m for Figure 2(b2) with $t = +18$ m for Figure 2(b3)). Also, as the duration threshold was increased, the composite evolution became increasingly similar to the 2013–2015 MHW event.

The relationship between Northeast Pacific MHW evolution and ENSO development is seen by plotting the composite evolution of the NEPac index against the corresponding Niño 3.4 index (Figure 2(c)). Each curve shows, for different duration thresholds (color shading), the concurrent evolution of these two indices, with time running counter-clockwise from −12 to 24 months. Four distinctive phases of MHW evolution are evident: (1) initial equatorial Pacific cold anomalies persist/strengthen as the MHW rapidly strengthens, crossing the 1σ threshold value at $t = 0$ (open circles); (2) subsequently, El Niño conditions develop, with relatively little change in MHW amplitude; (3) El Niño remains strong or even amplifies while the MHW gradually weakens; and (4) El Niño fades in the equatorial Pacific. These curves show that longer events start with colder Niño 3.4 values and (more slowly) develop warmer Niño 3.4 values, compared to shorter events, despite identical MHW intensity at $t = 0$. Overall, these results suggest a key tropical role in driving more persistent MHWs in the Northeast Pacific (Joh & Di Lorenzo, 2017; Liguori & Di Lorenzo, 2018), corroborating previous studies emphasizing how tropical teleconnections shaped the 2013–2015 MHW event (Capotondi et al., 2019; Di Lorenzo & Mantua, 2016).

We next examine additional factors that might impact intensity without impacting duration. Figure 3 shows results of varying intensity thresholds for fixed 6-month duration threshold. The PDF of intensities from the simulated MHW events that persisted for ≥6-month duration and had an intensity ≥1σ (Figure 3(a)) shows that the LIM simulation could generate MHWs with amplitudes even greater than observed in the past 70 years (maximum intensity up to 4.8°C). Composite MHW evolution was then determined for subsets with intensities ≥5/3σ (Figure 3(b1)), ≥2σ (Figure 3(b2)), and ≥7/3σ (Figure 3(b3)). Unlike the results for fixed intensity events of increasing duration, the evolving patterns of weaker and stronger events all look very similar, apart from an overall increased amplitude throughout the Northeast Pacific. Initial cold anomalies

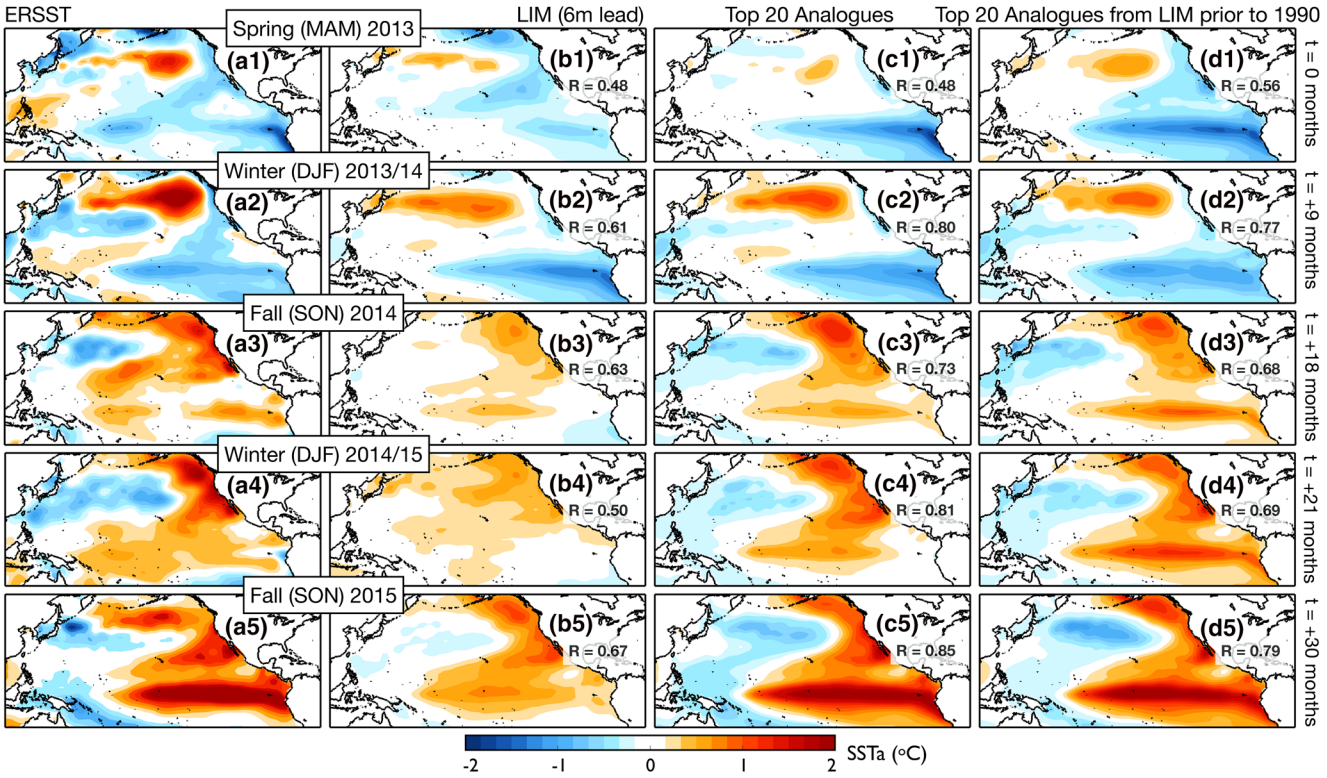

Figure 4. Evolution of seasonal SSTa, 2013–2015, from (a1-a5) observations, (b1-b5) 6-month lead cross-validated LIM predictions, (c1-c5) composite evolution of top 20 analogs of the 2013–2015 event within the LIM simulation, and (d1-d5) top 20 analogs from a separate LIM simulation built based on SSTa prior to 1990. (a1, b1, c1, d1) March–April–May (MAM) 2013. (a2, b2, c2, d2) December–January–February (DJF) 2014. (a3, b3, c3, d3) September–October–November (SON) 2014. (a4, b4, c4, d4) DJF 2015. (a5, b5, c5, d5) SON 2015.

in the equatorial Pacific were also almost identical (first and second rows of Figures 3(b1)–3(b3)), and the maximum El Niño warming occurred at about the same time (third and fourth rows of Figures 3(b1)–3(b3)), albeit the El Niño was generally warmer for higher MHW intensity thresholds. However, this relative tropical magnitude increase was less than the relative NEPac intensity increase. Similarly, the NEPac versus Niño 3.4 indices evolution curves (Figure 3(c)) demonstrate that increased MHW intensity depended more on the initial NEPac value than on the initial Niño 3.4 value. Overall, these results suggest that, for a given event duration, variations in MHW intensity may primarily result from initial conditions in the extratropics.

5. Implication for Understanding the 2013–2015 MHW Event

Finally, we evaluated how consistent the historic 2013–2015 MHW event is with the above LIM diagnosis, starting by analyzing its evolution and corresponding 6-month-lead LIM prediction (see Supplemental Material for LIM prediction). The observed evolution shows a large warm anomaly developing and then intensifying within the Gulf of Alaska, concurrent with a strengthening La Niña (Figures 4(a1) and 4(a2)). The warm SSTa subsequently spread eastward and along the entire Pacific North American coastal boundary, along with a meridional mode structure and weak positive tropical SSTa (Figures 4(a3)–4(a4)). The event ended with El Niño developing in the equatorial Pacific (Figure 4(a5)). Note that this evolution featured both long-lasting, record-breaking warm anomalies in Northeast Pacific and the delayed development of strong El Niño conditions. Based on our findings in Section 4, this extended duration may be largely attributable to the tropical variability, while the record-breaking intensity may be influenced by initial extratropical conditions.

The 6-month-lead LIM prediction patterns (Figures 4(b1)–4(b5)) track the observed evolution patterns (Figures 4(a1)–4(a5)) with significant spatial correlation skill ($R = 0.6$). Notably, the LIM predicted North

Pacific offshore warming in spring 2013 (Figure 4(b1)) and the intensification of the anomalies in winter 2013/14 (Figure 4(b2)). The NPMM-like warm anomalies with weak El Niño (Figures 4(b3) and 4(b_4)) in fall 2014 and winter 2014/15 and the emergence of El Niño in fall 2015 (Figure 4b5) were also predicted. Overall, these predictions again demonstrate the LIM's capability for capturing Pacific dynamics and seasonal MHW evolution.

While the statistical behavior of the MHW composite was captured by the ensemble LIM simulation, perhaps the 2013–2015 MHW event was too extreme for our simple stochastically forced linear model. Therefore, we explored whether a subset of MHWs in the LIM simulation could be found that represented this single historical event. Using an analog approach (e.g., Ding et al., 2018; Vandendool, 1994), we determined the 20 MHW events from the LIM simulation with the highest spatial and temporal correlation to the 2013–2015 MHW event over its *entire* 32 months evolution (see Supplemental Material). The composite of these "top-20" analogs (Figures 4(c1)–4(c5)) shows a similar evolution pattern to the 2013–2015 event ($R = 0.8$). However, the amplitudes are less extreme, suggesting the importance of noise to the evolution of any individual event.

Lastly, to evaluate whether our LIM ensemble was dependent upon possible climate change, we repeated the analysis by constructing a new LIM from data only over the interval 1950–1989, and then ran a separate ensemble LIM simulation. The "top-20" analog composite from the new ensemble LIM simulation (Figures 4(d1)–4(d5)) also captures the 2013–2015 event ($R = 0.7$), but its amplitudes are a little weaker, which can only partly be explained by sampling (not shown). The overall similarity of both composites suggests that the 2013–2015 event evolved in a manner consistent with Pacific climate dynamics prior to the emergence of any visible climate change effects in the North Pacific. However, the pre-1990 LIM cannot entirely capture such a prolonged period of high amplitudes, suggesting some potential climate change component that remains to be quantified.

6. Conclusions

Our study explored Northeast Pacific warming events over a continuum of intensities and durations, including the evolution of conditions as extreme as occurred during the 2013–2015 MHW, suggesting that these events are a recurrent phenomenon of North Pacific dynamics. Using the ensemble LIM simulation, we reproduced the statistics of observed MHWs, notably the relative frequencies of events with different durations and intensities and their corresponding composite evolution. The LIM large ensemble was then used to diagnose relative tropical and extratropical influences on MHW intensity and duration. We find that greater MHW duration is linked to stronger La Niña during the early stages of MHW evolution and to a subsequently extended development of El Niño, suggesting that the tropics play an important role in MHW duration. In contrast, MHW intensity depends primarily on North Pacific initial conditions, suggesting that MHW intensity may be largely driven by variability intrinsic to the extratropics. Both contributed to the multiyear persistence and record-breaking intensity of the 2013–2015 MHW event.

We did not address the potential role of climate change since our study was performed on linearly detrended observations. However, our analysis does suggest that the mean changes in SST due to recent climate trends in the North Pacific are not a necessary requirement to explain the evolution of an event like the 2013–2015 MHW. The analysis of the ensemble LIM analogs trained with data between 1950 and 1989 captures MHWs that are dynamically consistent with the 2013–2015 event. Nevertheless, climate change could still have been a contributing factor, particularly for the *prolonged severity* of the 2013–2015 MHW which is not fully captured by our analysis. Some recent studies (Laufkötter et al., 2020; Oliver, 2019) suggest that the main impact of climate change upon MHWs is through changing the mean rather than the variability, which is consistent with our approach. We could also address this issue in the LIM framework by exploring changes of the LIM itself, as done by Capotondi and Sardeshmukh (2017) for the tropical Pacific.

Data Availability Statement

Extended Reconstruction SST, version 3 (ERSST.v3b) data were obtained online from NOAA NCEI at https://www1.ncdc.noaa.gov/pub/data/cmb/ersst/v3b/netcdf/.

Acknowledgments
The study was supported by Department of Energy (grant #0000238382). Dr. Antonietta Capotondi was supported by the NOAA Climate Program Office Modeling Analysis Prediction and Projection Program. The authors thank Dr. Kevin Haas at the Georgia Institute of Technology for his financial support. The authors thank reviewers for their insightful comments.

References

Alexander, M. A., Blade, I., Newman, M., Lanzante, J. R., Lau, N. C., & Scott, J. D. (2002). The atmospheric bridge: The influence of ENSO teleconnections on air–sea interaction over the global oceans. *Journal of Climate*, *15*, 2205–2231.

Alexander, M. A., Matrosova, L., Penland, C., Scott, J. D., & Chang, P. (2008). Forecasting Pacific SSTs: Linear inverse model predictions of the PDO. *Journal of Climate*, *21*, 385–402.

Amaya, D., Bond, N., Miller, A., & DeFlorio, M. (2016). The evolution and known atmospheric forcing mechanisms behind the 2013–2015 North Pacific warm anomalies. *CLIVAR's Variations Newsletter. Spring*, 1–6.

Amaya, D. J., Miller, A. J., Xie, S.-P., & Yu, K. (2020). Physical drivers of the summer 2019 North Pacific marine heatwave. *Nature Communications*, *11*, 1903.

Bond, N. A., Cronin, M. F., Freeland, H., & Mantua, N. (2015). Causes and impacts of the 2014 warm anomaly in the NE Pacific. *Geophysical Research Letters*, *42*, 3414–3420. https://doi.org/10.1002/2015GL063306

Capotondi, A., & Sardeshmukh, P. D. (2015). Optimal precursors of different types of ENSO events. *Geophysical Research Letters*, *42*, 9952–9960. https://doi.org/10.1002/2015GL066171

Capotondi, A., & Sardeshmukh, P. D. (2017). Is El Niño really changing? *Geophysical Research Letters*, *44*, 8548–8556. https://doi.org/10.1002/2017GL074515

Capotondi, A., Sardeshmukh, P. D., Di Lorenzo, E., Subramanian, A. C., & Miller, A. J. (2019). Predictability of US West Coast Ocean Temperatures is not solely due to ENSO. *Scientific Reports*, *9*, 10.

Cavole, L. M., Demko, A. M., Diner, R. E., Giddings, A., Koester, I., Pagniello, C. M. L. S., et al. (2016). Biological impacts of the 2013–2015 warm-water anomaly in the Northeast Pacific. *Oceanography*, *29*, 273–285.

Chiang, J. C. H., & Vimont, D. J. (2004). Analogous Pacific and Atlantic meridional modes of tropical atmosphere-ocean variability. *Journal of Climate*, *17*, 4143–4158.

Deser, C., Simpson, I. R., Phillips, A. S., & McKinnon, K. A. (2018). How well do we know ENSO's climate impacts over North America, and how do we evaluate models accordingly? *Journal of Climate*, *31*, 4991–5014.

Dias, D. F., Subramanian, A., Zanna, L., & Miller, A. J. (2019). Remote and local influences in forecasting Pacific SST: A linear inverse model and a multimodel ensemble study. *Climate Dynamics*, *52*, 3183–3201.

Di Lorenzo, E., & Mantua, N. (2016). Multi-year persistence of the 2014/15 North Pacific marine heatwave. *Nature Climate Change*, *6*, 1042–1047.

Ding, H., Newman, M., Alexander, M. A., & Wittenberg, A. T. (2018). Skillful climate forecasts of the tropical Indo-Pacific Ocean using model-analogs. *Journal of Climate*, *31*, 5437–5459.

Dole, R. M., & Gordon, N. D. (1983). Persistent anomalies of the extratropical Northern Hemisphere wintertime circulation—Geographical-distribution and regional persistence characteristics. *Monthly Weather Review*, *111*, 1567–1586.

Frankignoul, C., & Hasselmann, K. (1977). Stochastic climate models, Part II. Application to sea-surface temperature anomalies and thermocline variability. *Tellus*, *29*, 289–305.

Frolicher, T. L., & Laufkotter, C. (2018). Emerging risks from marine heat waves. *Nature Communications*, *9*, 4.

Hasselmann, K. (1976). Stochastic climate models. 1. Theory. *Tellus*, *28*, 473–485.

Hobday, A. J., Alexander, L. V., Perkins, S. E., Smale, D. A., Straub, S. C., Oliver, E. C. J., et al. (2016). A hierarchical approach to defining marine heatwaves. *Progress in Oceanography*, *141*, 227–238.

Hobday, A. J., Oliver, E. C. J., Sen Gupta, A., Benthuysen, J. A., Burrows, M. T., Donat, M. G., et al. (2018). Categorizing and naming marine heatwaves. *Oceanography*, *31*, 162–173.

Holbrook, N. J., Gupta, A. S., Eric, C. J., Oliver, A. J., Hobday, J. A., Benthuysen, H. A., et al. (2020). Keeping pace with marine heatwaves. *Nature Reviews Earth & Environment*, *1*, 482–493.

Holbrook, N. J., Scannell, H. A., Sen Gupta, A., Benthuysen, J. A., Feng, M., Oliver, E. C. J., et al. (2019). A global assessment of marine heatwaves and their drivers. *Nature Communications*, *10*, 13.

Hu, Z. Z., Kumar, A., Jha, B., Zhu, J. S., & Huang, B. H. (2017). Persistence and predictions of the remarkable warm anomaly in the Northeastern Pacific Ocean during 2014–16. *Journal of Climate*, *30*, 689–702.

Jacox, M. G., Alexander, M. A., Bograd, S. J., & Scott, J. D. (2020). Thermal displacement by marine heatwaves. *Nature*, *584*, 82–86.

Jacox, M. G., Tommasi, D., Alexander, M. A., Hervieux, G., & Stock, C. A. (2019). Predicting the evolution of the 2014–2016 California current system marine heatwave from an ensemble of coupled global climate forecasts. *Frontiers in Marine Science*, *6*, 13.

Joh, Y., & Di Lorenzo, E. (2017). Increasing coupling between NPGO and PDO leads to prolonged marine heatwaves in the Northeast Pacific. *Geophysical Research Letters*, *44*, 11663–11671. https://doi.org/10.1002/2017GL075930

Jones, T., Parrish, J. K., Peterson, W. T., Bjorkstedt, E. P., Bond, N. A., Ballance, L. T., et al. (2018). Massive mortality of a planktivorous seabird in response to a marine heatwave. *Geophysical Research Letters*, *45*, 3193–3202. https://doi.org/10.1002/2017GL076164

Larson, S. M., & Kirtman, B. P. (2014). The Pacific meridional mode as an ENSO precursor and predictor in the North American multimodel ensemble. *Journal of Climate*, *27*, 7018–7032.

Laufkötter, C., Zscheischler, J., Thomas, L., & Frölicher (2020). High-impact marine heatwaves attributable to human-induced global warming. *Science*, *369*, 1621.

Liguori, G., & Di Lorenzo, E. (2018). Meridional modes and increasing Pacific decadal variability under anthropogenic forcing. *Geophysical Research Letters*, *45*, 983–991. https://doi.org/10.1002/2017GL076548

McCabe, R. M., Hickey, B. M., Kudela, R. M., Lefebvre, K. A., Adams, N. G., Bill, B. D., et al. (2016). An unprecedented coastwide toxic algal bloom linked to anomalous ocean conditions. *Geophysical Research Letters*, *43*, 10366–10376. https://doi.org/10.1002/2016GL070023

Miller, R. L., Lackmann, G. M., & Robinson, W. A. (2020). A new variable-threshold persistent anomaly index: Northern Hemisphere anomalies in the ERA-interim reanalysis. *Monthly Weather Review*, *148*, 43–62.

Newman, M., Alexander, M. A., Ault, T. R., Cobb, K. M., Deser, C., Di Lorenzo, E., et al. (2016). The Pacific decadal oscillation, revisited. *Journal of Climate*, *29*, 4399–4427.

Newman, M., Alexander, M. A., & Scott, J. D. (2011). An empirical model of tropical ocean dynamics. *Climate Dynamics*, *37*, 1823–1841.

Newman, M., & Sardeshmukh, P. D. (2017). Are we near the predictability limit of tropical Indo-Pacific sea surface temperatures? *Geophysical Research Letters*, *44*, 8520–8529. https://doi.org/10.1002/2017GL074088

Newman, M., Shin, S. I., & Alexander, M. A. (2011). Natural variation in ENSO flavors. *Geophysical Research Letters*, *38*, L14705. https://doi.org/10.1029/2011GL047658

Oliver, E. C. J. (2019). Mean warming not variability drives marine heatwave trends. *Climate Dynamics*, *53*, 1653–1659.

Oliver, E. C. J., Donat, M. G., Burrows, M. T., Moore, P. J., Smale, D. A., Alexander, L. V., et al. (2018). Longer and more frequent marine heatwaves over the past century. *Nature Communications*, *9*, 12.

Penland, C., & Matrosova, L. (1994). A balance condition for stochastic numerical-models with application to the El-Nino-Southern Oscillation. *Journal of Climate*, *7*, 1352–1372.

Penland, C., & Sardeshmukh, P. D. (1995). The optimal-growth of tropical sea-surface temperature anomalies. *Journal of Climate*, *8*, 1999–2024.

Ryan, J. P., Kudela, R. M., Birch, J. M., Blum, M., Bowers, H. A., Chavez, F. P., et al. (2017). Causality of an extreme harmful algal bloom in Monterey Bay, California, during the 2014–2016 Northeast Pacific warm anomaly. *Geophysical Research Letters*, *44*, 5571–5579. https://doi.org/10.1029/2017GL072637

Sanford, E., Sones, J. L., García-Reyes, M., Goddard, J. H. R., & Largier, J. L. (2019). Widespread shifts in the coastal biota of northern California during the 2014–2016 marine heatwaves. *Scientific Reports*, *9*(1), 4216. https://doi.org/10.1038/s41598-019-40784-3

Santora, J. A., Mantua, N. J., Schroeder, I. D., Field, J. C., Hazen, E. L., Bograd, S. J., et al. (2020). Habitat compression and ecosystem shifts as potential links between marine heatwave and record whale entanglements. *Nature Communications*, *11*(1), 536. https://doi.org/10.1038/s41467-019-14215-w

Scannell, H. A., Pershing, A. J., Alexander, M. A., Thomas, A. C., & Mills, K. E. (2016). Frequency of marine heatwaves in the North Atlantic and North Pacific since 1950. *Geophysical Research Letters*, *43*, 2069–2076. https://doi.org/10.1002/2015GL067308

Smith, T. M., Reynolds, R. W., Peterson, T. C., & Lawrimore, J. (2008). Improvements to NOAA's historical merged land-ocean surface temperature analysis (1880–2006). *Journal of Climate*, *21*, 2283–2296.

Vandendool, H. M. (1994). Searching for analogs, how long must we wait. *Tellus Series A: Dynamic Meteorology and Oceanography*, *46*, 314–324.